J Mater Sci (2006) 41:8031–8046
DOI 10.1007/s10853-006-0770-8

Role of ion depletion in the electrophoretic deposition of alumina powder from ethanol with increasing quantities of HCl

Jonathan J. Van Tassel · Clive A. Randall

Received: 17 January 2006 / Accepted: 7 August 2006 / Published online: 4 November 2006

Abstract Under certain conditions of conductivity and at constant current, electrophoretic deposition (EPD) of alumina powder from an acidic suspension is accompanied by an anomalous voltage rise across the deposited particulate layer. This voltage rise, which is much greater than can be accounted for by the blocking of the electrode by non-conducting particles, is the signal of the formation of a very uniform, dense alumina deposition layer. To determine the conditions necessary to induce this effect and discover its origins, a series of systematic EPD trials with increasing quantities of HCL is comprehensively examined. It is shown that both of these effects can be accounted for by the formation of an ion depleted conduction layer in the solvent at the deposition electrode, which is marked by extremely high voltage gradients. The resulting electrophoretic force on particles in this layer is several orders of magnitude higher than the force on particles in the rest of the system and consolidates the particles to form the observed densely compacted layer. This high voltage gradient layer also results in a significant self-leveling effect for deposition thickness. A complete description of the various types of deposition observed in this series of trials is then given in which EPD is treated as a series of three steps: accumulation, deposition, and consolidation. This description identifies the origin of several effects seen during EPD and is intended to help the reader identify the conditions necessary to induce ion depletion enhanced, automatic leveling electrophoretic deposition.

Abbreviations

DEBL	Diffuse electrostatic boundary layer, (double layer)
EPD	Electrophoretic Deposition
EHD	Electrohydrodynamic

Introduction

In the course of many various deposition experiments the authors have noted that when a deposition conducted at constant current is accompanied by a large linear voltage rise, the resulting deposition layer is especially uniform with a volume density 55–65%. This voltage rise occurs entirely within the deposited particle layer and is much higher than can be explained by simple blocking of the electrode by non-conductive particles. This voltage rise was first noted by Sarkar and Nicholson [1, 2]. To understand when and why this voltage rise occurs, and why it signals the formation of a dense, uniform, adherent deposition layer, this paper analyses in depth a series of deposition trials performed on a suspension of alumina particles in ethanol with increasing quantities of added HCl. Within these trials, three different types of behavior were noted and a trial from within each of these groups was taken for detailed analysis.

J. J. Van Tassel (✉) · C. A. Randall
Materials Research Lab, Penn State University,
University Park, PA 16802, USA
e-mail: vantassel@psu.edu

However, before any detailed discussion of EPD can occur, a great deal of relevant background material must be established. This is done in sections from ‘‘Experimental’’ to ‘‘Deposition and consolidation mechanisms,’’ with a specific discussion of the EPD results occurring only in section ‘‘Analysis of electrophoretic deposition results.’’ Section ‘‘Experimental’’ is a simple presentation of experimental procedure and results. Section ‘‘Suspension description’’ is an analytic description of the starting suspension, and presents data, which is used in the following sections. Much of this data comes from [3], and this reference will be very helpful to the reader interested in understanding the surface adsorption and surface charge formation on the alumina particles used in this experiment. Section ‘‘Conductivity, conduction, ionic concentration gradients and fluxes’’ is the largest and most critical section of the paper. It is a detailed analysis of ionic concentrations, gradients and fluxes, and the consequent changes in conductivity and voltage gradients when a constant current is driven through the system.

Conduction in a liquid only occurs by electrophoretic migration of ions through the solvent with oxidation/reduction reactions occurring at the electrodes. In the bulk solution, migration of positive and negative ions in opposite directions cancels, and ionic concentration remains unchanged. At the electrodes, however, the ionic concentration, and consequently conductivity, will either go up or down depending on whether ions are either generated or consumed in the electrochemical reactions at that electrode. In the case considered here positive ions are consumed at the deposition electrode (cathode), and negative ions migrate away from the cathode both due to the electric field and to maintain an electrostatic balance with the number or positive ions in solution. Thus the ionic concentration and conductivity will go down in a layer next to the electrode surface [4–6].

Without particles, this ionic depletion would proceed very rapidly to a point where the layer becomes unstable and convection begins. However, the presence of particles migrating to the cathode has a dramatic impact on the formation of these ionic concentration gradients. Electrophoretic migration of the particles has very little impact on net charge migration, i.e., conduction, but the large number of ions reversibly adsorbed to the surface of the particles acts as an ionic concentration buffer, reducing the speed of these changes by 2–3 orders of magnitude. This allows the particles, which accumulate at the electrode to stabilize an ion depleted conduction layer. This is a layer where charge is carried only by positive ions pulled through the layer by the extremely high voltage gradient necessary to maintain a constant current through the system. It is this layer, which is the source of the large voltage rises seen in this type of deposition.

In sections from ‘‘Effects of particles on conduction’’ to ‘‘Comparison of trials #16 and #20’’ the system is analyzed by a simple accounting of the ionic fluxes in and out of a control volume at the cathode surface. It is shown that in one case the ionic buffering effect of the particles prevents the depletion of ions at the surface and no high voltage layer forms. In the second case, the flux of ions out of the control volume can be accounted for by the formation of a concentration gradient layer and an ion depletion layer within the layer of particles accumulated at the electrode. The thickness of the ion depleted layer calculated in this manner is within 20% of the thickness of the observed dense deposition layer in this case. In the final case we show that ionic transport by particle migration is less than ionic transport by migration of ions in solution, therefore convection must begin in the bulk solution to provide adequate ionic transport across the system to maintain the constant current. Nevertheless, the large voltage gradients seen in this deposition trial indicate that an ion depleted conduction layer must still be stabilized within the particle layer at the electrode.

Section ‘‘Voltage rise versus deposition thickness’’ then assumes the existence of an ion depleted conduction layer and calculates the thickness of this layer for nine deposition trials based on ionic flux, positive ion mobility, and the observed voltage rise during deposition. Over the seven trials within the conductivity range where the ion depleted layer is expected to be contained within the accumulated particle layer, the resulting calculated ion depletion layer thicknesses correspond to the observed dense deposition layer thicknesses with a standard deviation of only 4%.

The force that is generated on the particles by the high electric field of the ion depleted conduction layer is then discussed in section ‘‘Force on the particles in the ion depleted layer’’. Section ‘‘Deposition and consolidation mechanisms’’ describes very briefly the mechanisms of EPD relevant for this experiment.

Finally, having covered the background topics of: stability, conduction, ionic gradients, and fluxes, voltage gradients, and electrostatic forces on the particles, Section ‘‘Analysis of electrophoretic deposition results’’ discusses the EPD and consolidation of the alumina particles from suspension. This section is much less densely quantitative and is intended to describe how the deposition process changes as the ionic concentration in solution is raised. It is shown how, for the simple system of alumina in ethanol, four different behavior regimes exist for EPD depending on the amount of added HCl.

Of the many effects and concepts discussed in this paper, the concept of primary importance is that of ‘‘Ion Depletion Enhanced’’ electrostatic deposition. This is one of the most important practical mechanisms for EPD both because it is one of the few mechanisms that can produce a dense deposition prior to drying and because it has an effective, inherent automatic leveling effect. This allows the reliable and repeatable production of uniformly packed, uniform thickness depositions even without perfect uniformity of electric field or suspension density in the deposition cell.

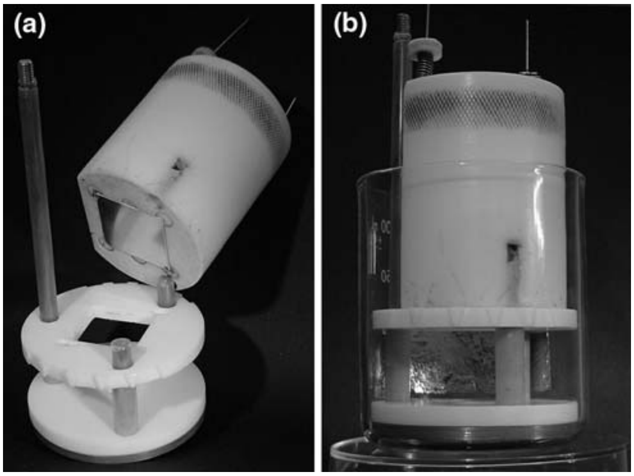

Fig. 1 Deposition Cell; (**a**) Device with holder block (upper) lifted from stand and masking disk (lower). Reflective square on the bottom of the holding block is the deposition electrode. (**b**) Assembled deposition device. One counter electrode is removed for clarity, second counter electrode is visible behind device stand

Experimental

Materials

The Al_2O_3 powder is AKP-50 from Sumitomo Chemical Co., Osaka, Japan. The number average particle diameter is 270 nm with a surface area of 10.0 m^2/g. The powder was washed and hydrated as described in [3]. Further details on materials, characterization, and preparation can also be found in Ref. [3].

Suspension preparation

Prior to mixing, the Al_2O_3 powder was placed in a 135 °C drying oven for at least 1 h to remove excess condensed moisture. About 7.99 g of this powder was added to 155.4 g of 99.5/0.5 wt.% ethanol/water in a HDPE bottle. This yields a 1.01 vol.% suspension of alumina particles based on an α-alumina density of 3.97 g/cc. 1 mm diameter alumina milling media was added, and the bottle was placed on a vibratory mill for 20 h to de-agglomerate the alumina particles. The suspension was then poured into another HDPE bottle through a sieve to remove the milling media prior to deposition trials. There was no evidence of remaining alumina sediment. Conductivity was measured at 0.1 μS/cm, the same as the as-received ethanol, indicating that no ionic contamination was added in this process.

Deposition device

The deposition trials were performed using a deposition device designed to be immersed in suspension in a 250 ml, 6.2 cm inside diameter Pyrex beaker, Fig. 1. The deposition electrode is a $25.4 \times 25.4 \times 0.5$ mm alumina circuit substrate with a sintered platinum coating on one side which was polished to a mirror finish. The deposition substrate is clipped to a PTFE holder block by two spring loaded stainless steel hooks which also serve to provide electrical connection to the platinum surface. The holder block is placed onto a 5 mm thick PTFE masking disk with a square cut-out which exposes a 5.2 cm^2 area of the deposition electrode. The mask disk is mounted horizontally on three posts above a cylindrical volume 1.5 cm high and 6 cm in diameter. The counter electrodes are two platinum foils which each cover one quadrant of the sides of this cylindrical volume. Deposition occurs in an upward direction.

During a deposition trial particles will move away from the counter electrodes. This creates an area of lower density fluid at the surface of the electrodes. The cell is designed so that this lower density, particle depleted fluid can rise to the surface of the suspension well above the electrophoresis zone. Undepleted fluid from below the surface of the suspension can then flow back down into the electrophoresis zone in the two quadrants not covered by the counter electrodes, replacing the depleted fluid. This flow pattern prevents gravitational convection or particle depleted solvent from the anode from affecting the deposition behavior at the cathode. In the center of the cylindrical volume the electrophoretic motion of the particles will become vertical, moving into the square mask cut-out toward the deposition electrode. Constant voltage/current is provided by a Keithly 2410 power supply, which also provided voltage/current measurements.

Conductivity measurement

Conductivity was measured using a voltage divider circuit with a 0.5 rms voltage at the conductivity probe. Oscillation frequency ranged from 100 Hz at the lowest conductivity to 2 kHz at the highest. The conductivity probe was a shiny platinum parallel plate design with a cell constant of 0.107 cm^{-1} (Orion Research, Inc., Beverly, MA). Accuracy is estimated to be the larger of ±0.2 μS/cm or ±5%.

Deposition procedure

The following is the step-by-step procedure for each deposition trial:

- 1 wt.% HCl solution in ethanol, if any, is added by weight. The suspension is stirred for at least 30 s, regardless of whether acid solution is added.
- Suspension conductivity is measured in the deposition cell.
- Deposition substrate is mounted on holding block and holding block placed on deposition device in the suspension.
- The power supply is turned on for approximately 1 s at 20 V and the current is recorded. The power supply is then switched to constant current mode and this current is entered so that each trial begins at ≈20 V.
- The power supply is then turned on for 120 s at constant current and the voltage recorded manually every 15 s.
- The mounting block and deposition substrate are then removed from the suspension and observed for deposition. The deposition substrate is removed from the mounting block with tweezers for rinsing. The deposition is exposed to air for approximately 10–15 s during this step. Although some evaporation occurs, no area of the deposition or substrate becomes dry prior to rinsing.
- The deposition substrate is rinsed in clear, as-received ethanol until no additional alumina is seen to rinse off the surface.
- The deposition is then allowed to dry and the weight is measured.
- The deposition substrate is then cleaned and the procedure repeated.

Data

This paper analyses a systematic series of 21 deposition trials performed on a single alumina suspension with increasing additions of HCl. As shown in Fig. 2 these depositions can be separated into four groups: depositions that occurred with no added acid, trials with small amounts of added acid where no depositions occurred, and two types of deposition at higher conductivities marked by significant voltage rises and dense deposition layers.

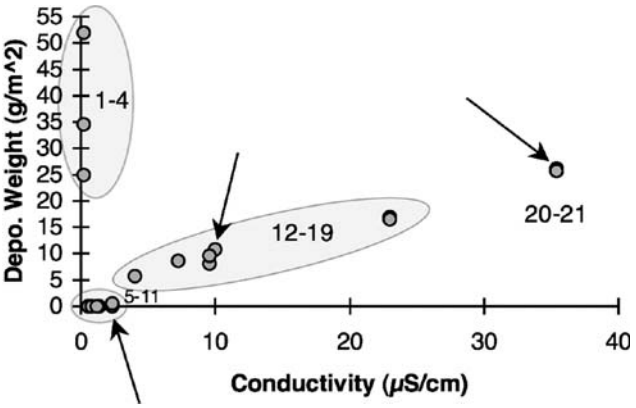

Fig. 2 Relationship between conductivity and deposition weight. Deposition trials can be separated into four groups. Arrows point to deposition trials 11, 16, and 20 chosen for detailed analysis

Deposition Trials 1–4—The first four deposition trials were performed on the as-prepared suspension containing only ethanol solution and alumina powder. Measured conductivity was 0.2 μS/cm. The current setting for deposition was 32.7 mA/m^2. Although depositions resulted from these trials, the results were very non-uniform. The voltage rises during deposition were 0.5, 2.0, 0.8, and 0.7 V. The first trial resulted in a thick, fluffy deposition covering most of the center of the electrode. The deposited area had irregular edges. Near the boundaries of the masked area there was no deposition. The unrinsed average deposition weight was 24 g/m^2. The second deposition covered the entire deposition area, however the entire deposition was removed by rinsing. During rinsing a distinct pattern in the deposition was observable, attributable to large scale convective motion of the suspension. The third deposition was very thick and appeared uniform prior to rinsing, however rinsing again revealed a distinct suspension flow pattern. Weight after rinsing was 53 g/m^2. The final deposition in this set again yielded a fairly uniform, low density deposition. The deposition weight without rinsing was 34 g/m^2. When the deposition was removed from the holder block and held at an angle the surface of the deposition was observed to flow as a high density slurry.

Deposition Trials 5–11—Deposition trials in this set conducted with progressively higher additions of HCl yielded no significant deposition. The first five trials in this set covered a conductivity range from 0.6 μS/cm to

Table 1 Deposition data

	Trial 11	Trial 16	Trial 20
Conductivity (μS/cm)	2.31	9.58	35.4
Current density (I) (A/m^2)	0.32	1.25	5.0
Total current (C/m^2)	38.3	150	600
Voltage rise (V)	1.0	3.3	18.9
Deposition weight (g/m^2)	0.6	8.1	26.1
Deposit specific current (C/g)	66	18	23
Deposition thickness at 60 vol.% density (μm)	0.24	3.4	11.0

1.2 μS/cm, showed voltage rises from 0.2 V to 0.7 V, and resulted in no deposition. The final two deposition trials were conducted at a conductivity of 2.3 μS/cm and showed voltage rises of 1.0 V and 1.1 V. A very small deposition of particles was observed in these cases as a slight fogging of the reflective platinum surface. The deposition weight of 0.6 g/m^2 corresponds to a uniform monolayer of particles. The final deposition trial of this set, #11, was chosen for detailed analysis in the following sections. The data for this trial is given in Table 1 and the voltage rise is shown in Fig. 3.

Depositions 12–19—This set of trials was marked by significant voltage rises during deposition, an overlayer of particles, which rinses off the substrate, and a uniform, dense deposition layer which does not rinse off. In these cases there is a clear distinction between the overlayer, which rinses off with little or no agitation, and the remaining dense deposited layer, which can only be partially removed by a solvent jet or ultrasonic agitation and can only be completely removed by mechanical scrubbing. No evidence of convection patterns was seen in the remaining deposited layer.

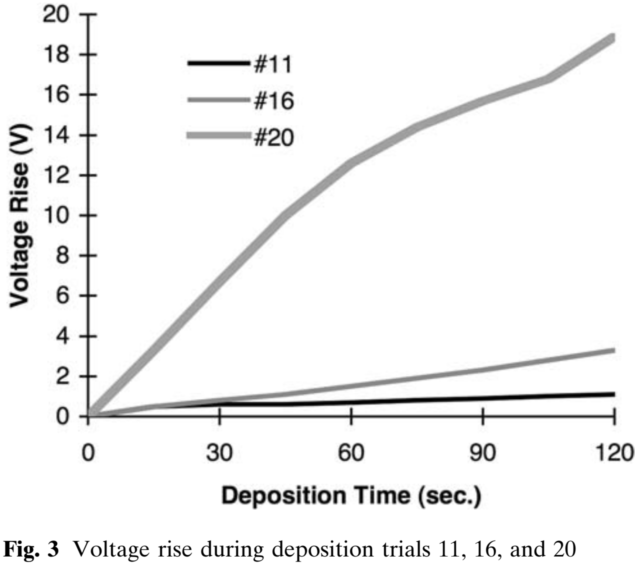

Fig. 3 Voltage rise during deposition trials 11, 16, and 20

Conductivities in this set range from 4.4 μS/cm to 23.0 μS/cm. Voltage rises were linear and increased with conductivity from 2.0 V to 14.0 V. Deposition weights also increased with conductivity from 5.8 g/m^2 to 26.1 g/m^2. A deposition from the middle of this set, #16, was chosen for detailed analysis.

Depositions 20–21—This pair of trials conducted at 35.4 μS/cm showed a non-linear voltage rise, which was nearly identical for both trials, Fig. 3. The distinction between rinsable overlayer and strongly deposited layer is less distinct, as progressively less alumina is rinsed off as the rinsing end point is reached. Again, the rinsed deposition was dense and uniform with no visible convection patterns. Of this pair, deposition #20 was chosen for detailed analysis.

Conductivity versus DC Conduction—The procedure above, section ‘‘Deposition procedure,’’ resulted in a linear relationship in all trials between measured conductivity and the current necessary to achieve a 20 V initial voltage.

Additional experimental data

Although this paper focuses on a particular set of depositions, these depositions represent only a very small set off all depositions of this type conducted. Two findings from these additional depositions are used here. Deposits, marked by a rise of several volts during deposition and which cannot be removed even by vigorous agitation during rinsing, were examined in cross-section by SEM of and found to have a density between 55% and 65%. Based on this, a density estimate of 60 vol.% is used here. A slightly higher or lower actual density will not significantly affect the conclusions reached here.

The second fact used here is the location of the excess voltage that arises during deposition. Experiments using a platinum wire as a voltage probe have shown that the voltage rise during deposition is almost completely accounted for by a potential difference across the deposited layer. For example, a constant current deposition with an initial potential of 20 V shows a rise in voltage to 40 V over the course of the deposition. The final voltage breakdown will be approximately: 20 V due to resistance of the solution, 1 V additional concentration potential across the bulk solution, and 19 V across the deposited layer. The wire probe can be pressed against the deposited layer, and, as long as the deposited particles are not scraped away, a 19 V potential difference will be measured between the deposition electrode and the solvent side of the deposition. This behavior is consistent with the observations previously reported by Sarkar and Nicholson [1, 2].

Suspension description

The properties of the suspending solvent and electrolyte are given in Table 2. The properties of the particles in suspension are given in Table 3. These values are calculated from the data presented in Ref. [3]. The net electrostatic charge is calculated using the estimation formula of Loeb et al. [7]. The particles are electrostatically stabilized by a repulsive osmotic pressure when they approach each other to the point that their diffuse electrostatic boundary layers (DEBL's) overlap.

From the data above it is possible to estimate the interaction potential of two average diameter spherical particles. These are shown as a function of separation distance for 270 nm dia. particles in Fig. 4. The attractive London-van der Waals force is calculated as outlined in Ref. [8]. This is adjusted for retardation of the interaction as separation distance increases using the estimation method of Russel et al. [9]. The repulsive force that results from the overlap of the DEBL's is calculated using the Derjaguin approximation for constant potential

$$\Phi = 2\pi\varepsilon_{\mathrm{r}}\varepsilon_{\mathrm{O}}\Psi_{\mathrm{O}}^{2}a\ln(1+\mathrm{e}^{-\kappa h})$$

from Ref. [9]. *a,* Particle radius (m); *h*, Particle–particle separation distance (m); ε_r, Relative dielectric constant; ε_o, Permittivity constant (C/V m); κ^{-1}, Debye length (m); Φ, Particle–particle interaction energy due to overlap of DEBL's (J); ψ_o, Potential at inside surface of DEBL (V). The total interaction energy is then the sum of these two forces.

To obtain an order-of-magnitude estimate of the electric field that would be necessary to bring two particles together, the maximum interparticle repulsion force was divided by the charge on a single average particle to obtain the voltage gradient that would

Table 2 Ionic properties of solution

	Trial 11	Trial 16	Trial 20
Conductivity (μS/cm)	2.31	9.58	35.4
Molar conductivity (Λ) (cm^2/Ω mol)	51.3	49.9	47.1
Bulk HCl concentration (mol/m^3)	0.045	0.192	0.751
Hydrogen ion mobility (v_{H}^{+}) (m^2/V s)	3.13×10^{-8}	3.04×10^{-8}	2.87×10^{-8}

Table 3 Surface and colloid properties

	Trial 11	Trial 16	Trial 20
Debye length (κ^{-1}) (nm)	26	12.5	6.3
Diffuse layer thickness index (κa)	5.24	10.8	21.4
Electrophoretic mobility (μm cm/V s)	0.97	0.85	0.47
Surface potential (mV)	79	51	26
Ave. particle electrostatic charge (C)	2.52×10^{-16}	2.64×10^{-16}	2.40×10^{-16}
Surface adsorbed HCl (μmol/g)	21.4	27.5	31.6

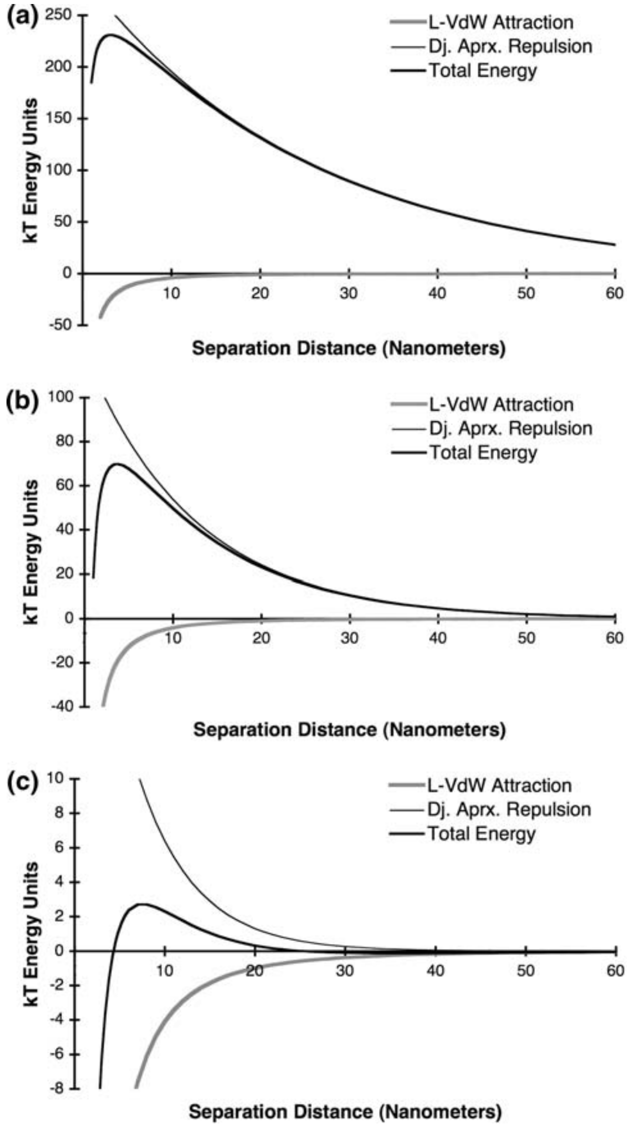

Fig. 4 Calculated electrostatic stabilization energies for suspension in; (**a**) trial 11, (**b**) trial 16, (**c**) trial 20

Table 4 Particle interaction properties

	Trial 11	Trial 16	Trial 20
Max. energy barrier to flocking (kT)	230	70	3.5
Max. interparticle repulsion force (pN)	28.2	15.5	1.42
Electric field to produce an equivalent force (V/cm)	1,120	590	60
Initial voltage gradient at depsition electrode (V/cm)	13.9	13.0	14.1

produce an equivalent force on an isolated particle, independent of electrohydrodynamic (EHD) effects. These values are shown in Table 4. Note that the electric field necessary to deposit the particles by direct electrostatic force alone is considerably higher than the actual bulk electric field in every case.

Conductivity, conduction, ionic concentration gradients, and fluxes

Electrode electrochemical boundary layer

Electrochemical conduction at the cathode occurs by the reduction of protonated ions, hydronium, and ethoxonium, to hydrogen and water or ethanol. As positive ions are consumed at the electrode negative ions will migrate away from the cathode in the applied electric field. This will result in an electrochemical boundary layer characterized by a reduction in the ionic concentration at the electrode [4–6, 10]. In the absence of particles the ionic concentration at the surface will reach a theoretical zero concentration 0.6 s after the current is turned on. (A version of the equation for quasi-neutral, constant current ion depletion at an electrode can be found in [11].) At this point a significant unbalanced electrostatic charge would develop causing the solution to immediately transition to convective motion in the electrochemical boundary layer. If this electroconvective motion begins, uniform EPD will not be possible.

Equilibrium limit current thickness

In 1959 Levich [4] clearly described the properties of the maximum limit current that can be conducted through a quasi-neutral electrolyte solution in the absence of convective motion. In this classic work, it was shown that at this limit current the ionic concentration gradient would decline linearly from the electrode where ions are generated to zero concentration at the electrode where ions are consumed.

The analysis here will use the inverse concept of the "equilibrium limit current thickness." This is the maximum thickness, d_{lim}, of an electrolyte layer that can conduct a given current flux.

$$d_{\mathrm{lim}} = \frac{2D_{\mathrm{H}} + c_{\mathrm{o}}}{J}$$

Here c_{o} is the maximum concentration, $D_{\mathrm{H}}+$ is the diffusion coefficient for the consumed ion in a 1–1 electrolyte and J is the molar current flux.

Effect of particles on conduction

The most important effect of the addition of particles to this system is the change of ionic transport and the buffering of ionic concentration changes during D.C. conduction. This result is counterintuitive because of the negligible effect the particles have on conductivity and conduction. As noted in [3], the difference in conductivity of a solution with 1 vol.% of particles either suspended or sedimented out was less than the margin of error in the conductivity measurement. Taking the net positive surface charge on the particles and the migration velocity of the particles in a D.C. electric field, the contribution to current flux in the bulk solution for the three cases here is 1.9, 0.4, and 0.06%.

However, when the total reversibly adsorbed HCl on the particle surfaces is considered, the picture is entirely different, Fig. 5a. The dissolved HCl in solution in these three cases is 0.045, 0.192, and 0.751 mol/m^3. The available HCl on the surfaces of the suspended alumina at the particle density of the bulk suspension is 0.865, 1.11, and 1.28 mol/m^3. This means that, per unit volume, the amount of HCl, which can desorb from the particle surfaces is 20, 6, and 2 times larger than the concentration of HCl in solution. This applies to the molar flux of HCl as well. Taking the migration speed and concentration of the alumina particles in the bulk solution, the total flux of HCl carried by the particles is 11.7, 12.3, and 8.47 μmol/s m^2 toward the cathode. This compares to the flux of dissolved chloride ions away from the cathode of 1.36, 5.32, and 21.3 μmol/s m^2.

Comparison of trials #11 and #16

To begin, the focus will be on deposition trials numbers 11 and 16. The objective will be to show why there is deposition accompanied by a stable linear voltage rise in trial #16 and no voltage rise or deposition in #11.

Ionic migration in the bulk suspension—In the solution without particles, an ionic concentration

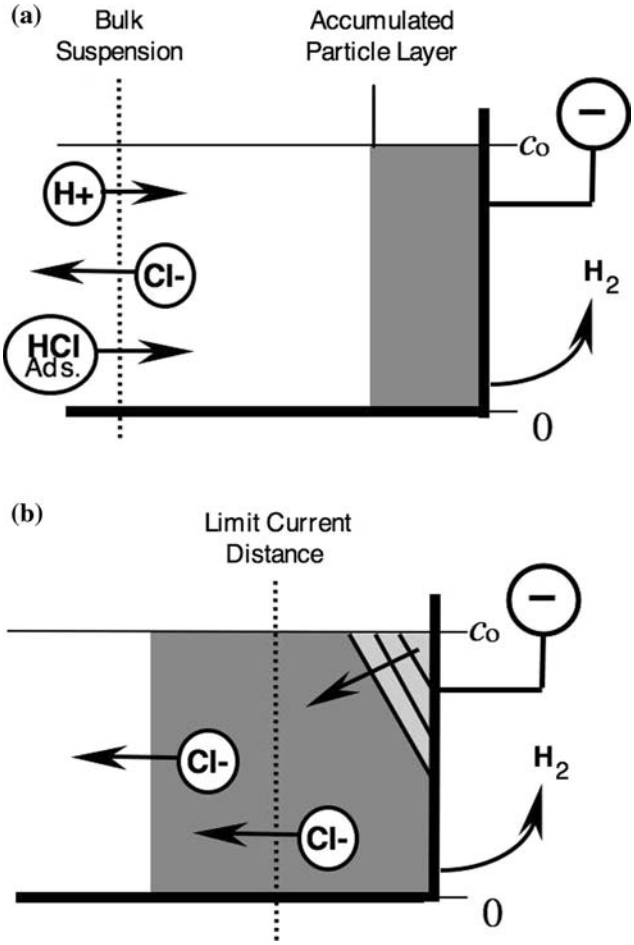

Fig. 5 In the bulk solution Cl^- migration is counteracted by electrophoretic motion of adsorbed HCl. At the cathode electrophoretic motion of the particles is stopped, but migration of Cl^- in solution continues

gradient forms at the cathode as H^+ ions are consumed and Cl^- ions migrate away faster than they are replenished by diffusion from the bulk. With particles present, the migration of Cl^- ions away from the electrode will be countered by the electrophoretic migration toward the electrode of adsorbed Cl^- ions on the particles. In both cases #11 and #16, the flux of adsorbed Cl^- carried by the particles is greater than the migration of dissolved Cl^-. Wherever the particles are free to move by electrophoresis no large ionic concentration gradients would be expected to develop. Up to the surface of the accumulated particle layer at the electrode the ionic concentration in solution will be the same as the bulk.

Accumulated layer—When the particles come up against the electrode, electrophoretic motion stops. Where the electrophoretic migration is stopped, the flux of adsorbed Cl^- becomes zero while the migration of Cl^- in solution continues, Fig. 5b. It is in this area that concentration gradients can develop.

Owing to the fact that there are no direct measurements of this layer, it is necessary to make some assumptions about the accumulation of particles at the electrode. In the bulk electric field of 13.9 V/cm in trial #11 the alumina particles will migrate at a speed of 13.5 μm/s. At the electrode the particles will accumulate at an estimated density of 20–25 vol.% based on an average interparticle separation of 80–90 nm, Fig. 3. This estimated density is very approximate, and there will most likely be a density gradient through this accumulated layer, however, the conclusions reached here will be valid for a wide variation in this density. At an average density of 25% the accumulated particle layer will grow at a rate of 0.375 μm/s, giving a total thickness of 45 μm over the 120 s of the deposition experiment.

In deposition trial #16 an accumulated layer density of 35% will be assumed. The reason for this higher assumed density is given in section ‘‘Analysis of electrophoretic deposition results.’’ In the bulk electric field of 13.0 V/cm the particles will migrate at a speed of 11.0 μm/s, accumulating a 38 μm layer over the 120 s deposition time.

Assumed gradient—Accurately modeling the development of these concentration gradients will likely require numerical simulation at some future date. However, by making some simplifying assumptions it is possible to establish a rough numerical criterion for what type of gradients will develop and when deposition of the particles will or will not occur. It is then also possible to qualitatively describe the development and shape of the concentration and potential gradients in this accumulated layer without the simplifying assumptions.

The greatest simplification can be made by replacing the actual non-linear adsorption isotherm with a simple linear adsorption for each of the cases. This is shown as the grey lines in Fig. 6.

The second assumption is that ionic concentration in solution is small relative to the adsorbed HCl in the accumulated layer. The implication of this second assumption is that desorption of HCl largely compensates for the consumption of H^+ at the cathode and the migration of Cl^- away. This means that the overall motion of the gradient layer will be slow relative to the movement of ions within the gradient layer. This then leads to the concept of the quasi-static, quasi-neutral gradient layer. In the Levich limit current case the migration of ions is blocked by the electrode at one end of the electrochemical cell, resulting in a constant ionic concentration at that point. In this case the desorption

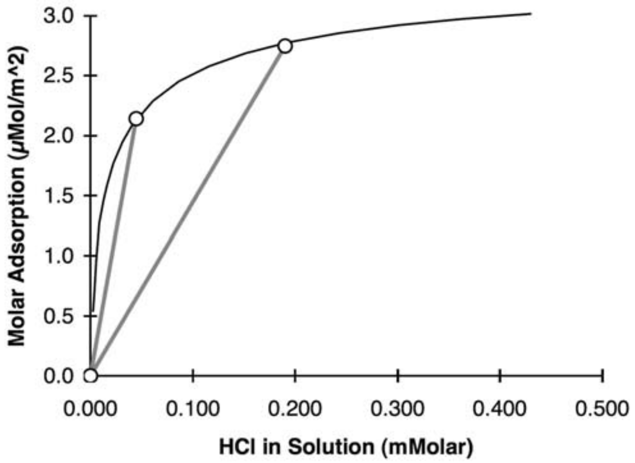

Fig. 6 Adsorption isotherm for HCl on alumina. Circles show the total adsorption for cases 11 & 16. Gray lines show the linear adsorption assumption. Black line is modified linear assumption for case 16

of HCl does not result in a fixed concentration but one that changes relatively slowly. Owing to this slow change in concentration and therefore slow movement of the gradient layer, we approximate the behavior of a stationary gradient layer (quasi-static) with the equation from Levich [4] for a stationary limit current gradient. This means that a linear concentration gradient layer is assumed with a slope equal to the slope in the limit current case, declining from a point where the concentration is equal to the bulk solution to a lower concentration at the electrode.

The ionic concentration gradient in the accumulated layer will then develop as shown in Fig. 7. A gradient with a constant slope will form at the cathode and will move slowly away as the adsorbed HCl in the layer next to the electrode is desorbed and consumed. Only when the edge of the gradient layer has moved to the limit current distance from the electrode will the concentration at the electrode drop effectively to zero allowing a charge depleted conduction layer to form, and it is only the formation of a charge depleted conduction layer that can account for the large voltage rises seen in the deposition trials.

This analysis is then turned around to define a criterion for the formation of a charge depleted layer. A control volume is defined which is bounded on one side by the electrode and on the other by an imaginary plane at the limit current distance from the electrode. If the net flux of Cl^- out of this volume is more than 1/2 of the Cl^- within this volume then a charge depleted layer can be expected to form.

Applying this criterion to deposition trials #11 and #16 clearly shows the difference between the two. In #11 the limit current distance is 22 μm. Since electrophoresis of the particles over the course of this trial results in an accumulated layer of approximately 45 μm, the control volume can be assumed to be completely filled by particles at a volume density of 25%. This then gives a total content of HCl, both adsorbed on the particles and in solution of 476 μmol/m^2. The flux of dissolved Cl^- out of this volume would be 1.36 μmol/s m^2, or only 163 μmol/m^2 over the 120 s of this trial. This is only 35% of the Cl in the control volume, therefore in this case the presence of reversibly adsorbed HCl on the surface of the particles will suppress the formation of a charge depletion layer. Little or no voltage rise would be expected. This is shown is Fig. 6a.

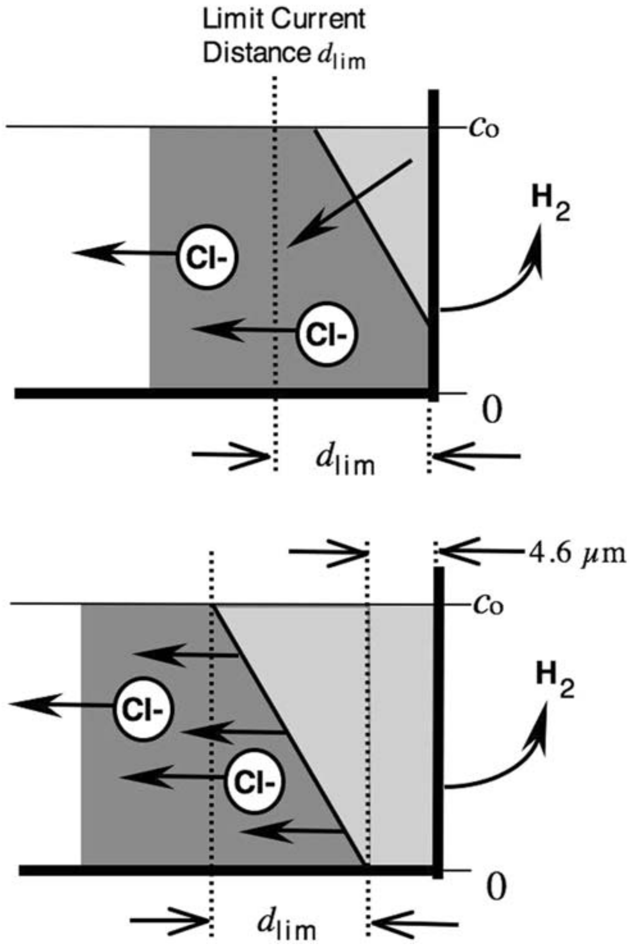

Fig. 7 (**a**) In deposition trial #11 the total Cl^- flux out of the control volume is less than 1/2 of the total content. (**b**) Trial #16 gradient layer moves away from electrode creating ion depleted layer

In the case of trial #16 the limit current thickness is 23 μm. Again this volume will be more than filled by particles due to electrophoresis during the deposition trial. This then gives a total content of HCl in the 23 μm control volume of 895 μmol/m^2. The molar flux of Cl^- out of this volume is 5.32 μmol/s m^2, or 628 μmol/m^2 over the course of the trial. This clearly exceeds the criterion set out above of 1/2 the molar contents of the control volume. In this case an ion depleted layer would be expected to develop. This is also consistent with the 3.3 V rise actually seen during this deposition trial.

Assuming a constant gradient moves from the cathode, the total outward flux of Cl^- ions could be accounted for by desorption from a 23 μm gradient layer and a 4.6 μm thick charge depleted layer, Fig. 6b. This 4.6 μm is calculated based on the 35 vol.% particle density assumption for the accumulated layer. If this 4.6 μm layer is consolidated to 60 vol.% by the high electric field in the depleted layer, the resulting layer would be 2.7 μm. This is only 20% less than the actual deposition thickness of 3.3 μm.

Comparison of trials #16 and #20

While the picture given above for deposition in trial #16 is complex, the evolution of the deposition process during trial #20 becomes even more so. In deposition trial #11 the accumulation of particles at the electrode suppressed the formation of a high voltage gradient and no deposition occurred. In deposition trial #16 the flux of Cl^- on the particles toward the electrode was higher than the migration of Cl^- ions in solution away from the electrode. This means that high voltage gradients could only form within the accumulated particle layer. Adsorption equilibrium within this layer suppresses convective motion, and analysis based on ionic migration alone can account for the observed behavior.

In deposition trial #20, on the other hand, the molar flux of Cl^- ions in solution away from the cathode is 21.3 μmol/s m^2 while the flux of Cl^- on the particles toward the electrode is only 8.5 μmol/s m^2. Without convection there would be a total flux of Cl^- ions away from the electrode of 2,500 μmol/m^2. The total Cl^- quantity available in the region next to the electrode from desorption and solution depletion is only 1,000 μmol/m^2. The remaining 1,500 μmol/m^2 can only be accounted for by convective flows, which wash Cl^- ions from the bulk back toward the cathode. This means that the particles will neither suppress the formation of an ion depletion region, nor will they contain this region within the layer of accumulated particles at the electrode surface and thereby suppress convection.

However, to account for the 18.9 V rise in cell voltage over the course of this deposition trial the particles must stabilize an ion depleted layer. Therefore, a stabilized ion depletion layer within the accumulated particle layer must co-exist with electroconvection in the bulk solution.

Based on the particle mobility in the bulk electric field of 14.1 V/cm, without convective motion an accumulation of 31.7 g/m^2 of particles at the electrode would be expected. The weight of deposited particles after rinsing was 26.1 g/m^2 or 80% of the particles that would be expected to accumulate at the electrode. During rinsing however a substantial overlayer of very loosely deposited material was removed. The densely deposited layer, which could not be removed by rinsing will have a volume density of 50–60%, giving a thickness of 11–13 μm. Thus in this case there is the same structure of a loosely deposited and rinsable overlayer and a dense deposited layer.

This structure will make sense if the system is made up of two layers, an ion depleted conduction layer next to the cathode, covered by an ionic gradient/buffer layer which is stabilized by the immobile deposited particles. On the solution side of this layer the ionic concentration will fluctuate somewhat due to electroconvective motion of the bulk suspension, but will remain high enough that voltage gradients in solution do not rise significantly. Through this buffer layer ionic concentration will decline and voltage gradients rise up to the edge of the ion depleted layer. Sitting between a semi-constant concentration on the solution side and an effectively zero concentration on the ion depleted side, the ionic concentration gradient in this layer will approach the Levich limit current case and the thickness of this layer will be a stable function of ion flux.

Thus in the case of Trial 16 there will be an ion depleted conduction layer growing through the accumulated particle layer, with that growth regulated by ionic flux out of the accumulated layer. In the case of Trial 20, the growth of the ion depleted conduction layer is limited by the rate, which the gradient/buffer layer moves away from the cathode, which is the speed of growth of the accumulated particle layer.

Voltage rise versus deposition thickness

Throughout the previous discussion it was assumed that the anomalous voltage rise seen in the cases where a deposition formed was due to the formation of an ion depleted conduction layer. If this is correct then some correlation would be expected between the estimated ion depletion layer thickness and the deposition thickness.

The first step is defining the anomalous voltage. Deposition trials #5 through 9 had an average voltage rise of 0.4 V. Deposition trials #10 & 11 showed the deposition of a monolayer of particles accompanied by voltage rises of 1.0 V and 1.1 V. Based on these observations it will be assumed that 1 V of the voltage rise during deposition can be attributed to voltage necessary to drive a direct current through the solvent (concentration polarization) and to voltage rise due to blocking of the electrode surface by deposited particles. The anomalous voltage is then taken as the voltage rise above one volt over the course of a deposition trial.

An ion depleted layer thickness can then be generated based on this anomalous voltage and the ionic flux density by using the equation for the potential drop across an unbalanced charge conduction layer, from Ref. [5].

$$\phi = -\frac{2}{3}\left[\frac{2JF}{v_{\mathrm{H}} + \varepsilon_{\mathrm{r}}\varepsilon_{\mathrm{o}}}\right]^{\frac{1}{2}} x^{\frac{3}{2}}$$

F, Faraday Constant; *J*, Ionic flux (mol/s m^2); *x*, Thickness of ion depleted conduction layer (m); ε_r, Relative dielectic constant; ε_o, Permittivity constant; v_H, Hydrogen ion mobility (m^2/V s); ϕ, Voltage drop across ion depleted conduction layer (V).

The calculated ion depleted conduction layer thickness for each deposition trial from 12 to 21 is shown in Table 5 followed by actual deposition thickness based on a 60 vol.% density. The correlation is almost perfect for depositions 12–19 with a standard deviation of only 4%. For depositions 20 & 21 where convective motion in the solution is not suppressed, the calculated ion depletion layer is ≈30% less than the actual estimated thickness.

Force on the particles in the ion depleted layer

To appreciate the scale of the forces generated here, it is helpful to return to the force calculations for a particle under the conditions of deposition trial #16. As mentioned above the force on the particle in equilibrium electrophoresis in the bulk electric field is 3.4×10^{-13} N, which is equivalent to 840 times the force of gravity on the same size particle. The viscous force due to EHD flow in the opposite direction is then approximately 770 G in the opposite direction, giving a net force moving the particle through the solution of 70 G.

This would seem like a fairly substantial force until a comparison is made to the force that can be generated in the ion depleted conduction layer. As a particle moves through the quasi-neutral gradient region into the transition region the HCl on the particle will desorb, reducing the particle charge. However, as was shown in Ref. [3], in pure solvent the particle still has a significant positive charge of $\approx 4 \times 10^{-17}$ coulomb. Figure 8a shows the potential gradient next to the electrode after an approximately 3 μm charge depleted layer has developed. This shows the extent to which the potential gradient changes from the 13 V/cm of the bulk suspension. Figure 8b then shows the force that this electric field exerts on an average sized particle in this layer. One item to note is that in the charge depleted layer there will be no counter ions, therefore there will be no electrostatic boundary layer or electrohydrodynamic pumping of fluid away from the electrode to counter the direct electrostatic force. Hundred percent of this electrostatic force goes into compacting the particles in this layer. The second item to note is the sharp rise in the force on the particles. Although the actual shape of the voltage gradient in the transition region has not been solved here, it is clearly much less than a micron and is, in this case, on the same scale as the particles themselves. Despite the uncertainty about the exact shape of the transition region, it is possible to state that over a distance of two to three times the average particle diameter, the force on the particles will go up by an order of magnitude. This means that there can be a very sharply defined edge between a highly compacted deposition layer and an undeposited accumulated particle layer or a loose,

Table 5 Calculated ion depleted conduction layer thickness versus deposition thickness

Trial #[a]	Cond. (μS/cm)	Current (A/m^2)	Voltage rise (V)	Ion dep. cond. layer (μm)	Deposited layer thk. (μm)	Deviation (%)
12	4.4	6.25	2.0	2.3	2.4	–4
14	7.2	11.2	3.6	3.6	3.6	0
15	10	13.9	4.7	4.2	4.5	–6
16	10	12.5	3.3	3.2	3.4	–5
17	10	13.5	4.4	4.0	4.0	0
18	23	30.8	14.0	7.5	7.0	6
19	23	30.8	12.2	6.8	6.9	–1
20	35	50.0	18.9	7.9	10.9	–28
21	35	50.0	18.0	7.9	10.7	–26

[a] Deposition weight for trial #13 was not recorded

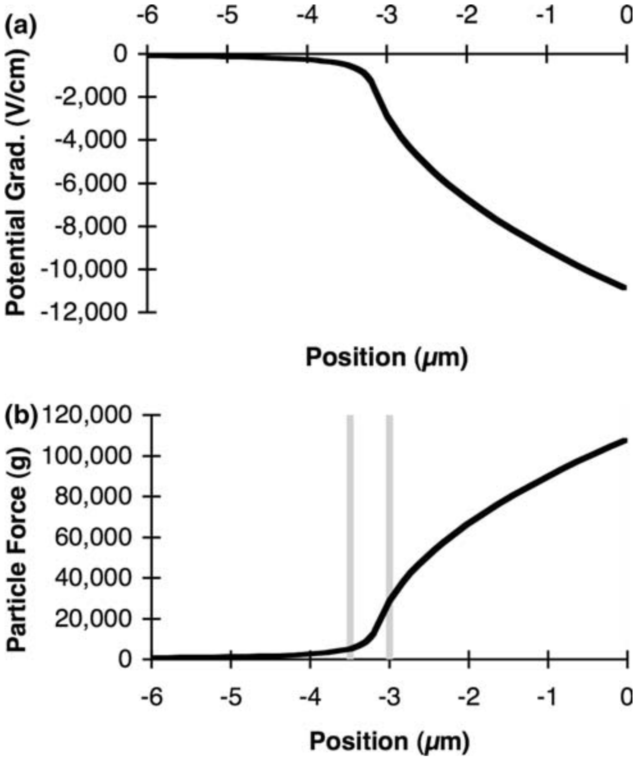

Fig. 8 (**a**) Potential gradient with 3 μm depleted layer for conditions of deposition trial #16, 0 position indicates electrode surface; (**b**) Electrostatic force on an average size particle in multiples of standard gravitational force on the same particle. Gray bars indicate approximate location of transition layer

low density deposited layer. Add to this the automatic leveling effect mentioned above and this mechanism can account for the thin, densely packed depositions with exceptionally uniform thickness that are frequently observed to be the product of a deposition accompanied by a linear voltage rise.

Deposition and consolidation mechanisms

This section briefly defines some of the mechanisms EPD and consolidation used in the following section to explain the observed depositions [12].

Electrostatic deposition—In this case the force of the external electric field acting on an undeposited particle is sufficient to overcome the interparticle repulsion causing that particle to come into contact with an already deposited particle, thereby becoming part of the growing deposition.

Electrosedimentary deposition—The electric field will pull on a particle which itself will not deposit, however, the repulsive force will push on a particle closer to the electrode. Eventually the force on a large enough stack of particles will cause the particle closest to the electrode to deposit. This mechanism of deposition was first proposed by Hamaker and Verwey in 1940 [13].

Convective deposition—This is the case where the hydrodynamic force of moving solvent can force particles into contact.

Electrosedimentary consolidation—Once deposition has occurred and the accumulated particle layer is no longer fluid, this problem is transformed into a problem of conduction through a particle bed. Example analyses of this problem in the case of equilibrium conduction can be found in [14–16]. The case here is somewhat different given that fluid motion is blocked at one side of the particle bed, but otherwise the same factors apply. The result is that there is a hydrostatic force on the entire layer as well as an electrostatic force on the particles in the layer. This combination of forces can consolidate what may begin as a low density deposition. Since the sum of these forces will increase with depth into the deposition this also can lead to a gradient of increasing density from the deposition surface to the electrode.

Ion depletion enhanced electrostatic consolidation—This is the result of the very strong electrostatic compaction force detailed in section ‘‘Force on the particles in the ion depleted layer’’ above.

Analysis of electrophoretic deposition results

With the background material established in the previous sections, it is finally possible to return to the description of the results that were obtained in this series of deposition trials with the object of offering a description of why these results were obtained.

Deposition trials 1–4—This set of trials was performed on a suspension with no added acid. As discussed in Ref. [3], the particles develop a positive 60 mV surface potential due to the dissociative adsorption of ethanol molecules and desorption of ethoxide ions. Due to the uncertainty of the actual ionic strength in the solution, the particle interaction force calculations are not shown here. However, knowing that the DEBL is thick and that the surface potential is relatively high allows two conclusions; a high surface potential means the energy barrier to flocking due to random motion is high and the thick boundary layer means that this interaction energy will be spread over a long distance leading to a low repulsive force. This means that the particles are well stabilized against flocking due to random motion in the quiescent solution but there is very little repulsive force resisting flocking by hydrodynamic or electrostatic forces.

When the current is turned on in these suspensions the solvent will rapidly transition to convection at the cathode. With no surface adsorbed ions the particles will have little effect on the development of ionic concentration and voltage gradients in the system. This convection was visible as the ripple patterns in all of the depositions, but is most obvious in the first deposition. Here inflowing suspension in the center of the deposition electrode allows a deposition to form while the balancing outflow of solvent at the edges of the electrode wash particles away leaving those areas bare.

The depositions that occurred in these four trials likely occurred by a combination of all three deposition mechanisms mentioned above. Convective deposition is a likely cause of the ridge patterns seen in the depositions when they are rinsed, but convective deposition cannot occur without some deposition occurring first by some other mechanism. The only other mechanisms available are electrostatic and electrosedimentary.

While convection may account for some deposition it is more likely to result in particles being washed away from the surface. Based on the bulk electric field and mobility of the particles, if the solvent were motionless and 100% of the particles accumulating at the electrode deposited, the expected deposition weight would be 54 g/m^2. This is very close to the actual deposition weight achieved in trial #3 of 53 g/m^2. However, that weight is after rinsing off a weakly deposited overlayer which would have raised the total weight well above expected. In contrast, deposition trial #4 yielded a deposition weight of only 34 g/m^2 even without rinsing. The wide scatter in deposition results in these four trials indicate the importance of the manner in which convection develops on the final deposition results.

After the particles have deposited on the surface of these depositions they appear to be subject to electrosedimentary consolidation. This would need to be confirmed by more careful future measurements of density gradients, but visual observation suggests that the deposition density increases continuously from the deposition surface to the electrode.

While depositions can be formed from this type of suspension, unless electroconvection can be precisely controlled, the deposits formed are unlikely to be uniform in thickness, density and total deposited weight, with low and fluctuating densities leading to severe cracking during drying.

Deposition trials 5–11—This set of deposition trials was performed on a series of suspensions where progressively more HCl was added to the solution. In this concentration range the majority of that added acid was adsorbed by the particle surfaces resulting in a large rise in the particle surface potentials. Enough of the HCl remains unadsorbed, however, that the free ionic content goes up and the DEBL thickness goes down. The higher potential creates a higher energy barrier to flocking by random motion, and the thinner diffuse layer means that this energy rise occurs over a shorter distance, meaning a much higher maximum repulsive force exists as well.

Even this dramatically increased stabilizing force could potentially be overcome if it were possible to develop the extreme voltage gradients associated with the ion depleted conduction layer. However, under the conditions of these deposition trials, the adsorbed HCl on the particles is too high and the current flux too low to allow these gradients to develop. The result is that no anomalous voltage rise occurred in this set of trials and no deposition occurred beyond a monolayer of particles.

Deposition trials 12–19—Although total surface charge on the particles does not change significantly over this set of trials, because of the increasing ionic concentration of the solution, the surface potential declines steadily as the DEBL gets thinner. These two effects lead to a decrease in both the total energy barrier to flocking and the maximum interparticle repulsive force. Nevertheless, in all of these suspensions the energy barriers and repulsive forces remain high and the suspensions exhibit long-term stability.

The most important change here from the previous set of deposition trials is the change in the ratio of conductivity to adsorbed HCl. In deposition trials 5–11 the quantity of HCl adsorbed to the particles rose much faster than the conductivity, so desorption from the particles was able to suppress the formation of an ion depleted layer. In this set of trials the adsorption is reaching saturation and the bulk of the HCl added at this point goes to increasing the conductivity of the solvent. With this increase in conductivity comes an increase in the current flux to maintain the same starting voltage. The flux of Cl$^-$ ions out of the accumulated particle layer is now sufficient to deplete the adsorbed Cl$^-$ on the particles next to the electrode, allowing an unbalanced charge conduction layer to form. Particles within this layer are compacted to almost maximum random packed density by the electrostatic force. This creates a dense, uniform deposition layer that is not removed by rinsing. That this layer is created by an ion depleted conduction layer is shown by the extraordinary match between estimated ion depletion layer thicknesses based on voltage rise and actual deposition thicknesses over this conductivity range, as shown in Table 5.

The ratio of conductivity to adsorption has not risen to the point that the flux of Cl^- ions in the bulk away from the cathode is greater than the flux of Cl^- adsorbed to the particles toward the cathode. This means that the electrophoresis of particles is able to suppress the formation of concentration gradient layers in the bulk solution that would drive EHD convection. Once the particles stop moving in the accumulated layer at the electrode they no longer prevent the formation of a ion depleted layer, but the large quantity of HCl that the particles can adsorb and release provides a vital role in stabilizing the ion depleted layer against convection within the accumulated particle layer. The high voltage gradient creates a strong automatic leveling effect for the ion depleted layer. This means that the dense deposited layer can be extremely uniform over a large area regardless of non-uniformities of the electric field in the bulk suspension.

The fact that the net flux of Cl^- ions in the bulk solution is toward the cathode means that particles will accumulate at the electrode faster than they are compacted into a dense deposition layer by the growth of the ion depleted layer. In the case of deposition trial #16, based on the particle mobility and bulk electric field the total particle accumulation at the cathode would be expected to be 53 g/m^2. Given the likelihood that convective motion of the suspension is suppressed, this estimate is likely fairly accurate. Of this only 8.1 g/m^2 is converted into a high density deposition. The balance is either not deposited at all or forms a weak, low density deposit which is easily rinsed off. The estimate of 35% density in this layer is based on both the interparticle interaction, Fig. 3, and the observed rinsing behavior of this layer.

The ratio of particle accumulation to deposition is a topic for future study, but the fact that a significant overlayer of particles (tens of microns) remains on the surface of the deposition electrode as it is removed from the deposition device and transferred to the rinse solution indicates that a significant portion of the accumulated particle layer does form a rigid deposition. The fact that it then easily rinses off indicates that this deposited layer has a very low density. Since the only two mechanisms for deposition in this layer are either electrostatic or electrosedimentary, it is possible to state that under these conditions, electrostatic stabilization with a DEBL thickness approximately 10% of the average particle radius, these mechanisms will not yield a densely packed deposition in the absence of the ion depletion enhanced electrostatic consolidation.

A very important feature of this type of deposition is a strong automatic leveling effect. The thickness of the ion depleted conduction layer is regulated by ionic flux. Since voltage drop is a function of thickness, in any areas where the ion depleted layer is relatively thinner there will also be a lower voltage drop across the layer. This means that at that point there will be a higher voltage gradient in the ionic gradient layer leading to faster outward migration of Cl^- ions. This causes faster growth of the ion depleted layer until the thickness is evened out. Likewise thicker areas will be evened out by slower growth. There is no mechanism to regulate the thickness of the accumulated particle layer, and the total thickness of the accumulated layer will be determined by convection and deposition cell geometry. However, if all of the particles outside of the ion depleted layer can be rinsed off, the result can be a very uniform deposition thickness even for complicated parts or non-uniform cell geometries.

Deposition trials 20–21—Although the estimated stabilizing energy barrier in these suspensions is low, the suspensions appear very stable with no visible sedimentation occurring over 8 h standing after the deposition trials were completed.

The primary difference between these two deposition trials and the previous set is the net Cl^- ion flux in the bulk solution. In the previous set of depositions the sum of the Cl^- ion migration in solution and Cl^- ion migration on the surface of the particles gave a net Cl^- ion flux toward the cathode. In these two trials conductivity has outstripped adsorption and the net Cl^- flux is now away from the cathode. This means that the particles will no longer contain the formation of steep gradient layers within the layer of accumulated particles at the electrode. The suspension outside of the accumulated particle layer will transition to convection.

The large voltage rises here show that this convection outside the accumulated layer does not prevent the formation and growth of an ion depleted layer. Since an ion depleted layer is extremely unstable in the absence of particles, there must be a layer of particles, which acts as a strong buffer between the unstable convection of the fluid suspension and the depleted layer.

The total deposition weight was 26.1 g/m^2. In the absence of convection, based on the particle mobility in the bulk electric field, an accumulation of 31.6 g/m^2 of particles would be expected. The weight of particles rinsed off of the deposition was not measured, but the quantity rinsed off appeared to be more than the 20%

discrepancy between these two numbers. This would suggest that electroconvective deposition was taking place, with convective flow accounting for the additional particle transport to create a thicker overlayer.

The most significant discrepancy is shown in Table 5. Based on the observed voltage rise, the ion depleted conduction layer would be expected to be ≈8 μ, while the depositions are approximately 11 μm thick. If the dense deposition and the depleted layer are the same thickness this would imply a higher than expected conductivity of this layer. Alternatively, part of the overlayer could be compacted to a sufficient density to resist rinsing. This could occur by electrosedimentary compaction, hydrodynamic compaction due to convective flows, or a high voltage gradient transition region in the buffer layer leading to electrostatic compaction. Determining which of these explanations is correct will require further experimentation and analysis.

This type of deposition will also exhibit a significant automatic leveling effect, although its method of regulation different from above. Where in trials 12–19 thickness is regulated by ionic migration, in 20–21 thickness is regulated by particle deposition. Because the motion of the gradient/buffer layer is limited by growth of the accumulated layer, in areas where the total layer is thinner, the ion depleted layer will be thinner as well. This means that there will be a higher voltage gradient in the suspension attracting more particles to the thinner area and thickness is regulated by particle deposition. This means that there will be an automatic leveling effect for the entire accumulated/deposited layer.

Conclusions

The objective of this paper has been to present a detailed analysis of a particular EPD system. A system was chosen which is known to produce good deposition results while being simple, stable, robust and reproducible. Alumina in ethanol with HCl has proven to be such a system. As shown in Ref. [3] the surface charge is uniformly positive and determined by a robust equilibrium between the solvent and Cl^- in solution. The suspension is stable over an easily measurable range of conductivities and has a window of conductivities where uniform, dense depositions can be reliably reproduced.

Here it is shown that the most significant effect of particles in this system is to change ionic transport in the solution and buffer ionic content changes at the electrode. As HCl is first added to the alumina suspension, most will be adsorbed to the particle surfaces with little remaining in solution to increase conductivity. As the particle surfaces become saturated, more and more of the added HCl will remain in solution and conductivity will begin to rise faster than total adsorption. This leads to three conduction regimes in this alumina/ethanol/HCl suspension:

1. *Convection-suppressed; depletion layer-suppressed*—In the low conductivity case, ionic flux in solution is small compared to the flux of adsorbed ions carried on the surfaces of the particles. This prevents significant ionic concentration gradients from forming and suppresses electrically forced convection. The large reservoir of adsorbed Cl^- in the accumulated particle layer at the electrode prevents the formation of a depleted layer over the time of this deposition.
2. *Convection-suppressed; depletion layer-stabilized*—In this higher conductivity case, the net flux of Cl^- ions in the bulk is still in the direction of the cathode, which suppresses EHD convection, but the higher ionic flux is sufficient to deplete the adsorbed ions in the accumulated layer at the electrode. An ion depleted conduction layer will form, a significant linear voltage rise is observed, and a dense, uniform deposited layer is formed.
3. *Convection-active; depletion layer-stabilized*—In this high conductivity case, the flux of dissolved Cl^- ions in the bulk away from the cathode is greater that the flux of adsorbed Cl^- on the particles moving toward the cathode. This means that ionic concentration gradient layers can form in the bulk solution, which initiate convection. Convection then provides the additional ionic transport necessary to maintain constant current in the cell. However, the buffering effect of particles in the accumulated layer at the electrode still allows an ion depleted layer to grow. The high response of adsorption to small changes in solution concentration at low concentrations means that the particles can stabilize an ion depleted conduction layer—even in the presence of fluctuating ionic concentrations at the surface of the accumulated particle layer due to unsteady convection in the bulk solution.

Finally, with a picture of ionic concentrations, voltage gradients, and convection states, it is possible to address the forming of a particulate deposition. Three mechanisms were presented as ways that particles in suspension could be forced into contact in the accumulated particle layer at the electrode: electrostatic, electrosedimentary, and convective deposition.

While these mechanisms alone were able to create a deposition which was rigid enough to be removed from the deposition solution and handled, these depositions were low enough density, and therefore of low strength, such that they could easily be rinsed off. The prerequisite for the formation of a densely packed deposition layer is the presence of an ion depleted conduction layer. It is only the extreme voltage gradients in this layer that exert sufficient force necessary to compact the particles to maximum density.

An additional benefit of this stabilized ion depleted layer is a strong automatic leveling effect. Owing to the voltage gradients in this layer are several orders of magnitude larger than in the bulk suspension, even a small irregularity in the thickness of this layer can lead to a large deflection of the bulk electric field, ionic flux and particle electrophoresis. All of these effects act to strongly damp any thickness variation in the dense deposited layer.

Since the ultimate objective of EPD is frequently to produce just these uniform thickness, densely packed layers of the particulate material, all of the various effects that occur in this type of deposition are collected under the name, ion depletion enhanced—automatic leveling deposition. Although the depositions made here were from an electrostatically stabilized suspension, this is not exclusive. Any set of deposition mechanisms [12] where the primary role of forming the dense deposited layer and defining its thickness is played by a stabilized ion depleted conduction layer would be included in this category.

Acknowledgements This work was funded by the Penn State Center for Dielectric Studies, the Penn State Particulate Materials Center, and the Intel Corporation.

References

1. Sarkar P, Huang X, Nicholson PS (1993) Ceram Eng Sci Proc 14:707
2. Sarkar P, Nicholson PS (1996) 62:271
3. Van Tassel JJ, Randall CA (2001) J Colloid Interface Sci 241:302
4. Levich VG (1962) Physicochemical hydrodynamics. Prentice-Hall, Englewood Cliffs, NJ
5. Chazviel J-N (1990) Phys Rev A 42(12):7355
6. Chu KT, Bazant MJ (2005) SIAM J Appl Math 65(5):1485
7. Loeb AL, Th J, Overbeek G, Wiersma PH (1961) The electrical double layer around a spherical colloidal particle. MIT Press, Cambridge, Massachusetts
8. Israelachvilli JN (1992) Intermolecular and surface forces. Academic Press, New York
9. Russel WB, Saville DA, Schowalter WR (1989) Colloidal dispersions. Cambridge University Press, Cambridge
10. De D, Nicholson PS (1999) J Am Ceram Soc 82(11):3031
11. Léger C, Elezgaray J, Argoul F (2000) Electroanal Chem 486:204
12. Van Tassel J, Randall CA (2006) In: Boccaccini AR, Van der Biest O, Clasen R (eds) Electrophoretic deposition: fundamentals and applications. Trans Tech Publications, pp 167–174
13. Hamaker HC, Verwey EJW (1940) Trans Faraday Soc 36:180
14. Rice CL, Whitehead R (1965) J Phys Chem 69(11):4017
15. Tavares MFM, McGuffin VL (1995) Anal Chem 67:3687
16. Wan Q-H (1997) Anal Chem 69:361